Hindawi Publishing Corporation
Journal of Nanomaterials
Volume 2014, Article ID 672798, 7 pages
http://dx.doi.org/10.1155/2014/672798

Research Article

Properties of Y-Shaped PFO-DBT Nanotubes

Muhamad Saipul Fakir, Azzuliani Supangat, and Khaulah Sulaiman

Low Dimensional Materials Research Centre, Department of Physics, University of Malaya, 50603 Kuala Lumpur, Malaysia

Correspondence should be addressed to Azzuliani Supangat; azzuliani@um.edu.my

Received 3 July 2014; Accepted 30 October 2014; Published 16 November 2014

Academic Editor: Zhi Li Xiao

Immersion of template into solution is used to synthesize the Y-shaped poly[2,7-(9,9-dioctylfluorene)-alt-4,7-bis(thiophen-2-yl)benzo-2,1,3-thiadiazole] (PFO-DBT) nanotubes. Solution annealing and different aging times (1, 24, and 72 hours) are conducted to synthesize the Y-shaped PFO-DBT nanotubes and the effects on the morphological, structural, and optical properties of Y-shaped PFO-DBT nanotubes are investigated. The dense, aligned, and elongated Y-shaped PFO-DBT nanotubes have been successfully fabricated by aging the PFO-DBT solution for 72 hours. Enhanced light absorption with less light scattering can be exhibited from the elongated Y-shaped PFO-DBT nanotubes. Partial and complete infiltration is governed by 1 hour and 72 hours of aging time, respectively. Preformed nanofibres are initiated by the process of annealing and aging of PFO-DBT solution. During the aging process, PFO-DBT nanofibres are formed to coat the pores' wall and replicated the Y-branched nanopores for the production of Y-shaped PFO-DBT nanotubes. The effects of solution annealing and aging process are essential for the improvement on the morphological, structural, and optical properties of Y-shaped PFO-DBT nanotubes.

1. Introduction

Recently, much consideration and attention have been given to the *p*-type semiconducting material of functional polymer in order to boost up the performance of organic electronics devices such as organic solar cells (OSCs), organic field effect transistors (OFETs), and organic light emitting diodes (OLEDs) [1–4]. One of the auspicious semiconducting polymers with the great optical properties is poly[2,7-(9,9-dioctylfluorene)-alt-4,7-bis(thiophen-2-yl)benzo-2,1,3-thiadiazole] (PFO-DBT). PFO-DBT or its derivatives have been widely used as the active layer in the optoelectronics devices and sensors [5–8]. The performance of these devices can be improved by modifying the morphological and optical properties of PFO-DBT that acts as an active layer. Novel nanostructured-based film is expected to heighten the sensitivity and the fast response time of sensors [9, 10]. Thus, studies on the synthesis of novel nanostructured-PFO-DBT based film should be given more attention in order to realize their significant potential in optoelectronic devices and sensors.

To consummate the synthesis of PFO-DBT nanostructures, a facile and contemptible method is rather indispensable. One of the reciprocal approaches is via template-assisted method. Template-assisted method is a substantial method due to its capability to produce a large scale of polymer nanostructure in one time of fabrication [11–13]. Different type of nanostructures can be produced depending on the technique that applied on the porous alumina template. As reported elsewhere, the nanoflowers [14], nanorods [15–17], and nanotubes [17, 18] can be synthesized via template-assisted method by implementing different deposition techniques such as spin-coated, dip-coated, melt-assisted, and drop-casted techniques.

Advancement in varying the deposition and infiltration techniques of template-assisted method is highly desired for the tunable parameters. One of the mutual advancements is by modifying the solution's condition. According to Collison et al. [19], the presence of "aggregates emission" of poly[2-methoxy-5-(2′-ethylhexyloxy)-p-phenylene vinylene] (MEH-PPV) solution is due to the effective conjugation length which leads to a spectral red shift in absorption and emission. Deposition of thin film via solution form can enhance its electroproperties by generating better interchain species during solution modification. Therefore, it is profitable for the solution to be modified before the deposition process.

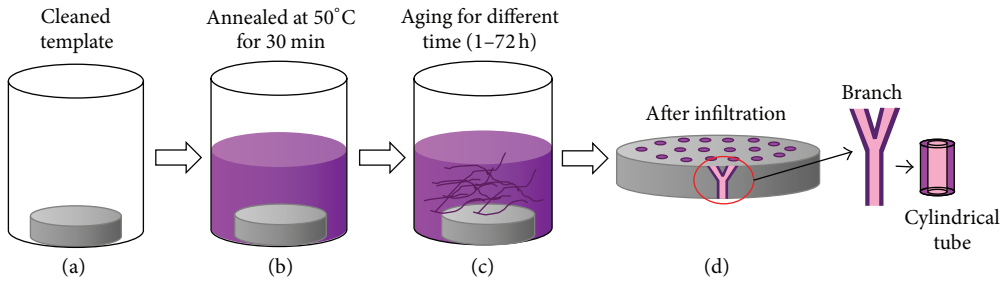

Figure 1: Schematic illustration of solution annealing and immersion process of PFO-DBT nanotubes.

Synthesisation of polymer nanowires and nanorods involving the cooling, heating, and aging processes in solution form has been narrated by some researchers [20, 21]. The interaction between solvent and chain segment of the molecule can be augmented with the incorporation of thermal energy which could increase the solubility of materials. Oh et al. [21] employed the heating and cooling of poly(3-hexylthiophene) (P3HT) which produce nanorods and nanofibrils at the room temperature. Annealing process has been known to improve the morphological and optical properties of polymer active layer [22]. Therefore, applying the prethermal treatment and aging time on solution is essential for the well-aggregated structure to form prior to the infiltration process.

By combining these two techniques, both the morphological and optical properties of PFO-DBT film can be improved. Therefore, the practical aim of this work is to investigate the effect of solution annealing and aging time on the properties of PFO-DBT nanotubes. Immersion technique of porous alumina template-assisted method is implemented by annealing the PFO-DBT solution and cooled it down at different aging times. PFO-DBT nanotubes consist of nanofibres that were preformed during the solution annealing.

2. Experimental Methods

Poly[2,7-(9,9-dioctylfluorene)-alt-4,7-bis(thiophen-2-yl) benzo-2,1,3-thiadiazole] (PFO-DBT) copolymer was obtained from Lum-Tec (Mentor, Oh, USA) and used without further purification. Using chloroform as the solvent, a 5 mg/mL of PFO-DBT solution was prepared. Anodic aluminum oxide (AAO) template with nominal pore diameter of 20 nm and thickness of 60 μm was purchased from Whatman Anodisc Inorganic Membrane (Sigma-Aldrich, St. Louis, MO, USA). The method for solution annealing and immersion process is simplified in Figure 1. Template was cleaned subsequently in deionized water and acetone for 10 minutes to remove any unwanted residual. After the cleaning and drying (with nitrogen) processes, the cleaned template was immediately placed in a vial (a). PFO-DBT solution was then placed in a vial together with the template prior to the annealing at 50°C (b). After 30 minutes of annealing, the template was left to cool at room temperature of different aging times (1, 24, and 72 hours) (c). The template was taken out from the vial and we let it dry after attaining the aging time (d). 3 M of sodium hydroxide (NaOH) was used to dissolve the template leaving the PFO-DBT nanotubes. The PFO-DBT nanotubes were purified in deionized water prior to the characterization.

The characterizations of PFO-DBT nanotubes were performed using field emission scanning electron microscope (FESEM) (Quanta FEG 450, Beijing, China), transmission electron microscope (TEM) (Tecnai G2 FEI, Tokyo, Japan), UV-Vis spectroscope (Jasco V-750, Tokyo, Japan), and photoluminescence spectroscope (RENISHAW).

3. Results and Discussion

Figure 2 shows the FESEM images of PFO-DBT nanostructures. It reveals that the structure formation is in nanometer scale with the Y-branched tube-like structure. After 1 hour of aging time, the solution has just started to infiltrate into the AAO cavity and is only capable to produce a shorter length of nanotubes (Figures 2(a) and 2(b)). The production of shorter nanotubes could be due to the insufficient infiltration time. Longer nanotubes are formed as the aging time is increased to 24 hours (Figure 2(c)). This result indicates that the length of the nanotubes is highly dependent on the aging time. This phenomenon supports the result of FESEM image shown in Figure 2(d). Aging time of 72 hours could provide farther aligned and dense Y-branched PFO-DBT nanotubes if compared with the shorter aging time (1 and 24 hours). On the contrary, solution annealing has no effect on the morphological properties of Y-branched PFO-DBT nanotubes as samilar morphological distribution between unannealed and annealed solution is observed. Instead of exhibiting the open-end PFO-DBT nanotubes arrays, PFO-DBT nanotubes grown by immersing the porous template have their tips fastening with each other as a result of van der Waals force attraction.

Figure 2(e) shows the cross-sectional view of porous alumina template that consists of Y-branched nanopores. The existence of Y-shaped PFO-DBT nanotubes (Figures 2(a)–2(c)) supports the primitive properties of Y-shaped nanopores (Figures 2(e)-2(f)). Y-branched PFO-DBT nanotubes exhibit ~250 nm in diameter which is comparable with the inner pore's diameter. During the aging time, the solution is infiltrated into the Y-shaped nanopores and replicated the pores to form "Y"-shaped nanotubes. If comparison is meant

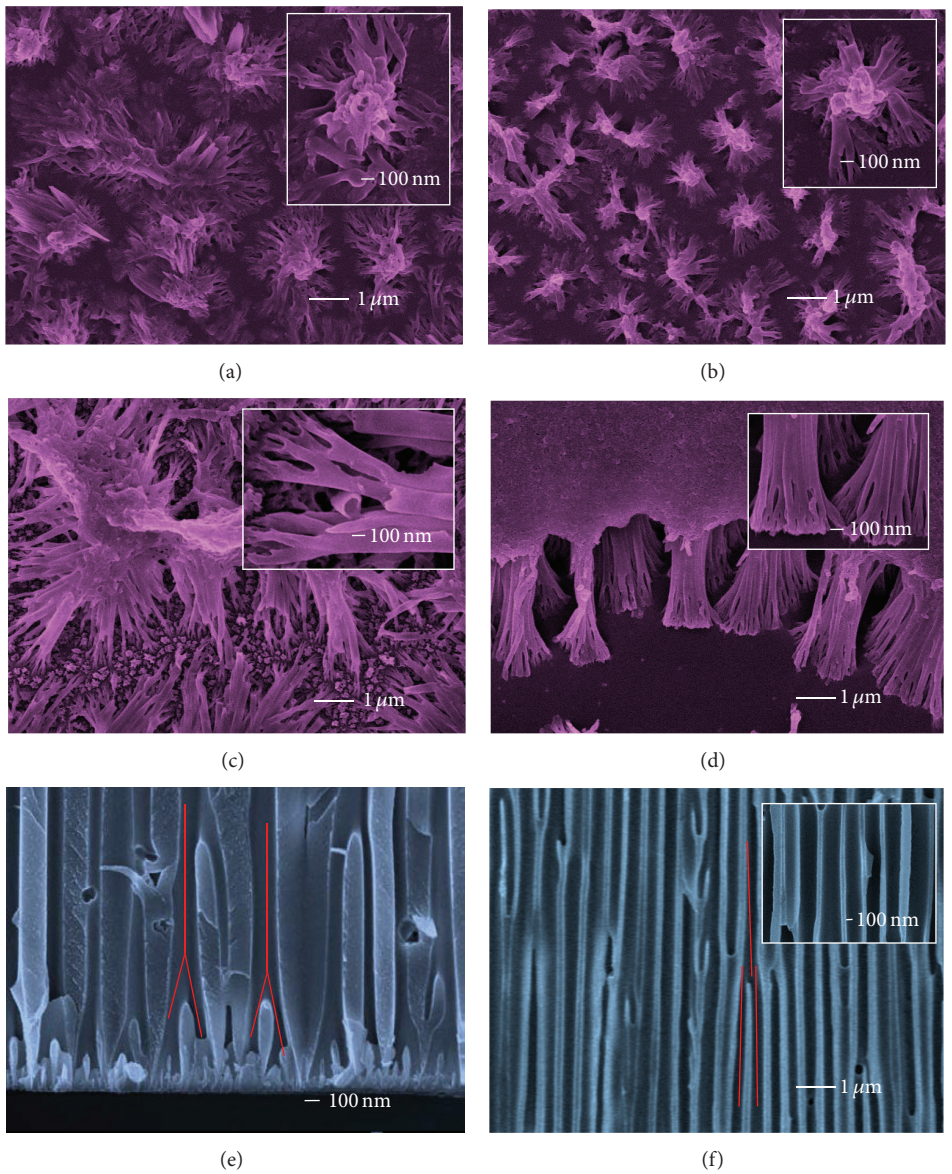

Figure 2: FESEM images of unannealed and annealed Y-shaped PFO-DBT nanotubes with different aging time. (a) Unannealed solution; (b) annealed solution of 1 hour aging time; (c) annealed solution of 24 hours aging time; (d) annealed solution of 72 hours aging time (insets show the enlarged respective images).

to be made between the aging time and the state of the nanotubes, Y-branched PFO-DBT nanotubes formed from the longer aging time are more ensembles due to the complete wetting process.

The effect of solution annealing on the structure of PFO-DBT nanotubes can be interpreted by the TEM images shown in Figure 3. As reported by Kim et al. and Oh et al. [20, 21], polymer nanowires can be created by annealing the polymer solution and aging it at certain times. The immersion of template into the annealed and aged PFO-DBT solution is expected to allow the infiltration of PFO-DBT nanofibres into the nanopores of AAO template. Formation of PFO-DBT nanotubes inside the confine nanopores may have been composed by nanofibres which then replicate the Y-branched nanopores. Figure 3(a) shows the formation of PFO-DBT nanotubes composed of nanofibres (red oval). The fragment observed in the background of nanotubes (Figure 3(b)) is depicted as PFO-DBT nanofibres. The rigorous TEM preparation has initiated to the broken, defected, and fractured nanotubes. Individual Y-branched PFO-DBT nanotube has been clearly seen in the TEM image (Figure 3(c)).

The infiltration of polymer solution into the Y-branched nanopores at different aging times is shown in Figure 4. Partial and complete infiltration has been seen to dominant the shorter and longer Y-branched PFO-DBT nanotubes, respectively. Sensibly, 1 hour of aging time will only instigate the infiltration process. The complete infiltration can only be achieved if sufficient aging time is employed. Dense and

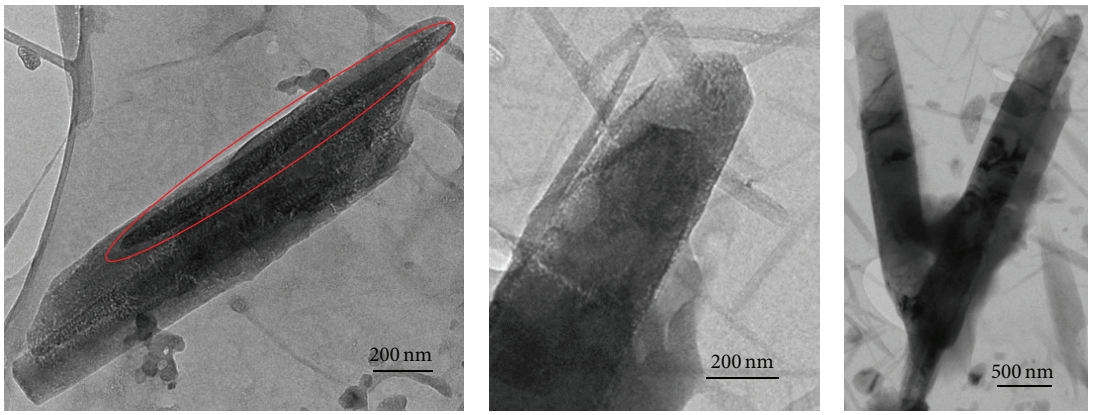

Figure 3: TEM images of PFO-DBT nanotubes. (a) PFO-DBT nanotubes composed of nanofibres (red oval). (b) Fragments of PFO-DBT nanofibres. (c) Y-shaped PFO-DBT nanotubes.

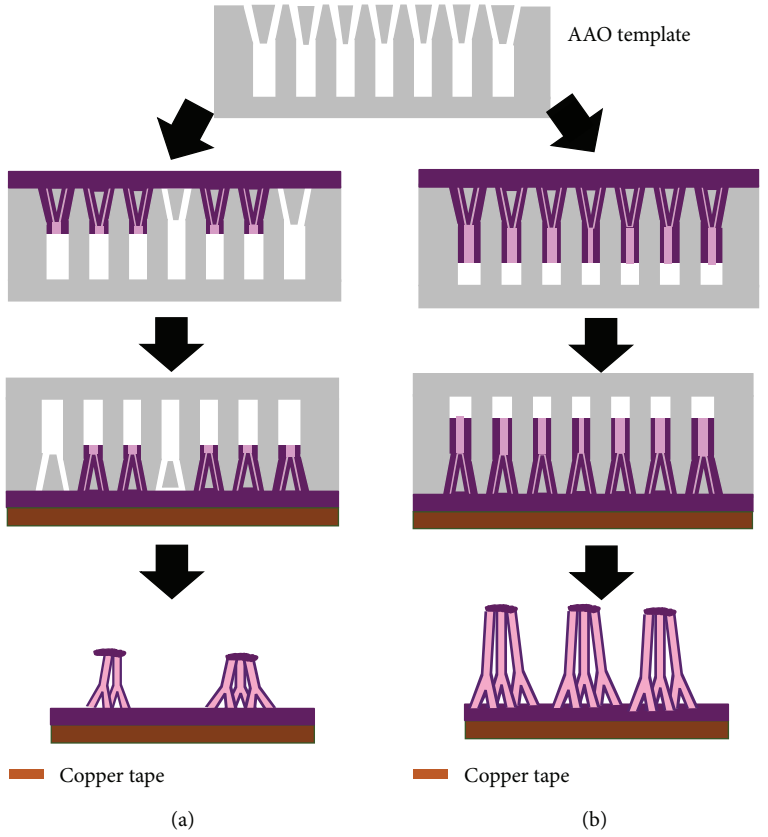

Figure 4: Schematic illustration of the infiltration process at different aging time. (a) 1 hour of aging time; (b) 72 hours of aging time.

aligned Y-branched PFO-DBT nanotubes are obtained from 72 hours of aging time.

Organic semiconductor material PFO-DBT constitutes dioctylfluorene and benzothiadiazole moieties. Thiophenes attached to the benzothiadiazole assist the moieties to absorb light with longer wavelength during the light absorption process. The light absorption properties of PFO-DBT moieties were depicted in Figures 5(a) and 5(b).

Two distinguished peaks are observed at B-band (short wavelength) and Q-band (long wavelength) which correspond to the absorption of dioctylfluorene [23] and the benzothiadiazole moieties assisted by the thiophene [24],

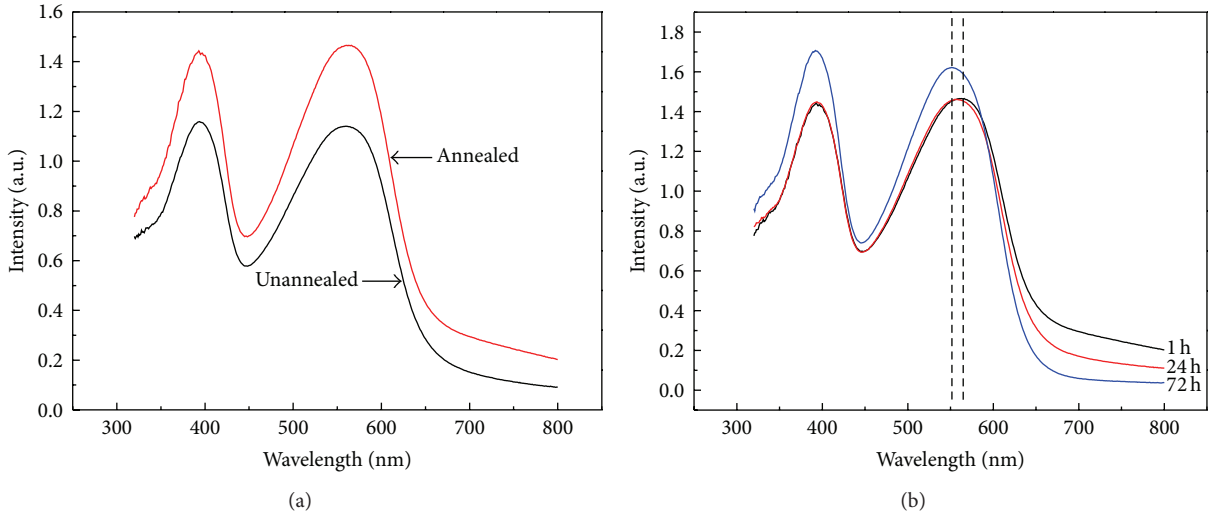

FIGURE 5: Optical absorption spectra of Y-shaped PFO-DBT nanotubes. (a) Absorption spectra of unannealed PFO-DBT solution (immersed for 1 hour) and annealed PFO-DBT solution (immersed for 1 hour). (b) Absorption spectra of annealed PFO-DBT solution of different aging time (1, 24, and 72 hours).

respectively. The peak absorption of B-band is detected at 392 nm and 557 nm for Q-band. In the normal circumstances, thermal treatment is performed to the organic thin film or solution with the purpose of improving the optical properties of the film [25]. By comparing the absorption spectra of annealed and unannealed solution with the template being immersed for 1 hour (Figure 5(a)), the annealed solution yields a higher light intensity at both peaks. This indicates that π to π^* transition of fluorine units of annealed PFO-DBT solution becomes stronger and efficient. The stronger and efficient transition may be due to the annealing effect which thus led to a better molecular arrangement. Further enhancement on the optical absorption properties of annealed solution is performed by increasing the aging time. By increasing the aging time, it allows the formation of nanofibres. During immersion, the solution with nanofibres is allowed to infiltrate into the cavity of porous alumina template and coated the wall. Varying the aging time will allow the solution to infiltrate deeper thus affecting the properties of the resulting nanotubes. As shown in Figure 5(b), an intense light absorption is observed from the 72 hours of aging time. However, it has exhibited a blue shift of 8 nm at the longer wavelength. The blue shift of the absorption peak could be due to the distortion of benzothiadiazole and thiophenes rings. Red shift at the peak absorption usually indicates the improvement of polymer conjugation length and chain alignment. However, as reported by Chirvase et al. [26], poly(3-hexylthiophene-2,5-diyl) (P3HT) has exhibited the blue shift due to the destruction of P3HT chain ordering. P3HT is an example of the semiconducting organic materials that consist of thiophenes. Correlation between the red and blue shift of P3HT and PFO-DBT can be realized due to the existence of thiophenes moieties in both semiconducting materials. Blue shift of PFO-DBT peak absorption is mainly caused by the distortion of benzothiadiazole ring. Since the Q-band corresponded to the benzothiadiazole and thiophene rings, the blue shift is merely affected by the distortion of both rings.

As depicted in Figure 6, the effect of solution annealing and different aging time is further characterized by photoluminescence (PL) spectroscopy. Occurrence of the red shift of PL emission is well matched with the red shift of UV-Vis absorption at the unannealed and annealed film. PL spectra for all conditions recorded an intense peak at 700 nm. An increase in intensity is observed for the annealed PFO-DBT solution (Figure 6(a)) which implies the segregation of PFO-DBT chain [26]. Chain segregation can occur by annealing the polymer solution where the process took place prior to the template immersion and infiltration. Segregated PFO-DBT chains have undergone the structural arrangements and led to the new channel of charge carriers' formation. These arrangements resulted from the thermal treatment process which could support a better photoinduced charge transfer within the PFO-DBT chain. As portrayed in Figure 6(b), the PL emission is quenched as the ageing time is increased.

In UV-Vis spectroscope, the light shone to the sample will absorb, transmit, or reflect. Light will scatter when there are irregularities in the propagating mediums or surfaces. Scattering process within the nanotubes that have been synthesized via the shorter and longer aging time is affected since their morphologies are unlikely to be similar. Light scattering can be affected by the available spaces within the hollow tubes and the standing ability or well-aligned nanotubes. As ascribed in UV-Vis absorption spectra, the absorption at the longer wavelength edge of the spectra which is due to light scattering became blue shifted as the aging time increased. To explain the effects of light scattering based on the changes of absorption edge in the UV-Vis spectra of Y-branched PFO-DBT nanotubes, schematic illustration diagram is proposed and presented in Figure 7. Shorter Y-branched PFO-DBT nanotubes due to the partial infiltration are mostly collapsed and thus will not be able to provide a

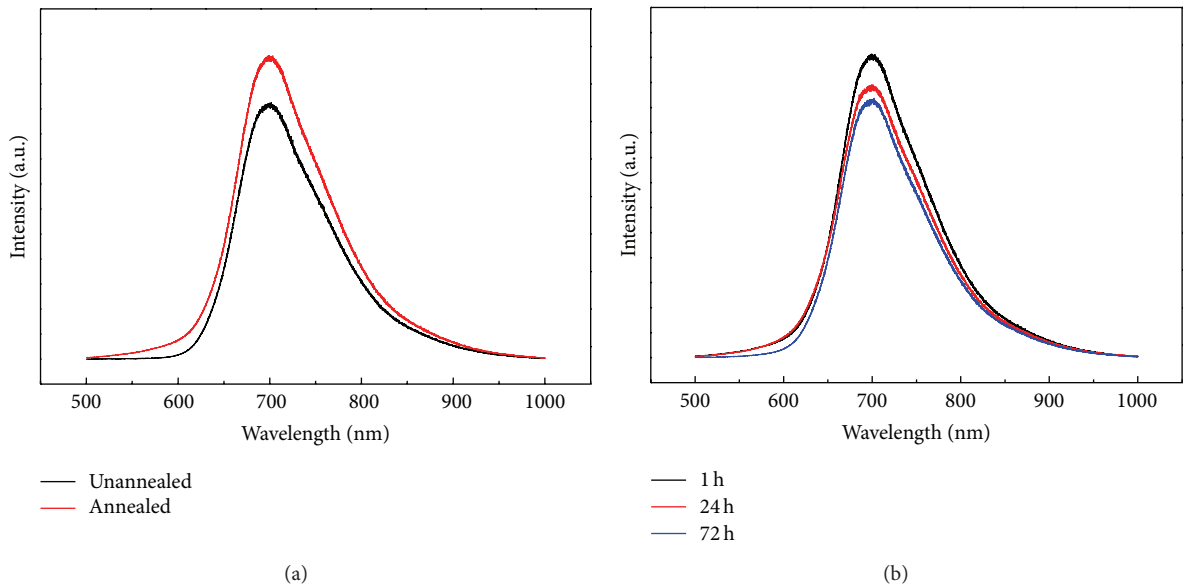

Figure 6: Photoluminescence spectra of Y-shaped PFO-DBT nanotubes. (a) PL spectra of unannealed PFO-DBT solution (immersed for 1 hour) and annealed PFO-DBT solution (immersed for 1 hour). (b) PL spectra of annealed PFO-DBT solution of different aging time (1, 24, and 72 hours).

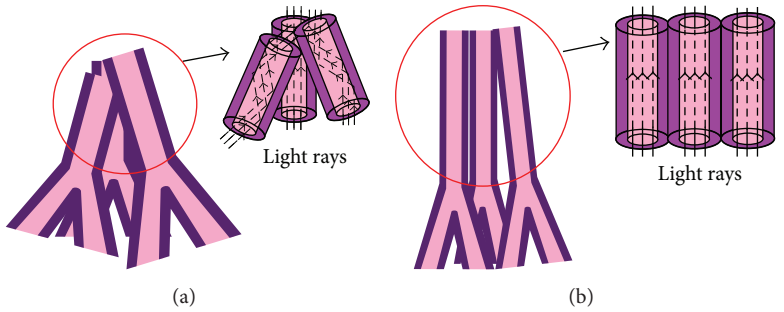

Figure 7: Schematic illustration of light scattering on Y-branched PFO-DBT nanotubes. (a) shorter aging time; (b) longer aging time.

pathway for the light to transmit. Most of the light will be reflected, diffused, and absorbed by the nanotubes which led to the intense light scattering (Figure 7(a)). Unlike the aligned Y-branched PFO-DBT nanotubes, transmission of light will likely occur and less light scattering is realized (Figure 7(b)). As the standing nanotubes provide an aligned empty space, it is easier for the light to pass through the nanotubes and reduce scattering effect.

4. Conclusions

In this work, Y-shaped PFO-DBT nanotubes have been synthesized using the template-assisted method. Effects of solution annealing and aging time on the morphological, structural, and optical properties of Y-shaped PFO-DBT nanotubes are discussed and reported. Preformed nanofibres are initiated by the process of annealing and aging of PFO-DBT solution. During the aging process, PFO-DBT nanofibres are formed to coat the pores' wall and replicated the Y-branched nanopores for the production of Y-shaped PFO-DBT nanotubes.

Conflict of Interests

The authors declare that there is no conflict of interests regarding the publication of this paper.

Acknowledgments

The authors would like to acknowledge the Ministry of Education Malaysia for project funding under Fundamental Research Grant Scheme (FP002-2013A) and the University of Malaya High Impact Research Grant UM-MoE (UM.S/625/3/HIR/MoE/SC/26).

References

[1] S. Günes, H. Neugebauer, and N. S. Sariciftci, "Conjugated polymer-based organic solar cells," *Chemical Reviews*, vol. 107, no. 4, pp. 1324–1338, 2007.

[2] H. Sirringhaus, "Device physics of solution-processed organic field-effect transistors," *Advanced Materials*, vol. 17, no. 20, pp. 2411–2425, 2005.

[3] H. Bronstein, Z. Chen, R. Shahid et al., "Thieno [3, 2-b] thiophe-ne—diketopyrrolopyrrole-containing polymers for high-performance organic field-effect transistors and organic photovoltaic devices," *Journal of the American Chemical Society*, vol. 133, no. 10, pp. 3272–3275, 2011.

[4] X. Zhou, J. Blochwitz, M. Pfeiffer et al., "Enhanced hole injection into amorphous hole-transport layers of organic light-emitting diodes using controlled p-type doping," *Advanced Functional Materials*, vol. 11, no. 4, pp. 310–314, 2001.

[5] H. Wang, Y. Xu, T. Tsuboi et al., "Energy transfer in polyfluorene copolymer used for white-light organic light emitting device," *Organic Electronics: Physics, Materials, Applications*, vol. 14, no. 3, pp. 827–838, 2013.

[6] E. Wang, L. Wang, L. Lan et al., "High-performance polymer heterojunction solar cells of a polysilafluorene derivative," *Applied Physics Letters*, vol. 92, no. 3, Article ID 033307, 2008.

[7] D. X. Zhu, H. Y. Zhen, H. Ye, and X. Liu, "Highly polarized white-light emission from a single copolymer based on fluorene," *Applied Physics Letters*, vol. 93, no. 16, Article ID 163309, 2008.

[8] J. Luo, X. Li, Q. Hou, J. Peng, W. Yang, and Y. Cao, "High-efficiency white-light emission from a single copolymer: fluorescent blue, green, and red chromophores on a conjugated polymer backbone," *Advanced Materials*, vol. 19, no. 8, pp. 1113–1117, 2007.

[9] S. Virji, J. Huang, R. B. Kaner, and B. H. Weiller, "Polyaniline nanofiber gas sensors: examination of response mechanisms," *Nano Letters*, vol. 4, no. 3, pp. 491–496, 2004.

[10] X.-J. Huang and Y.-K. Choi, "Chemical sensors based on nanostructured materials," *Sensors and Actuators B: Chemical*, vol. 122, no. 2, pp. 659–671, 2007.

[11] N. Haberkorn, J. S. Gutmann, and P. Theato, "Template-assisted fabrication of free-standing nanorod arrays of a hole-conducting cross-linked triphenylamine derivative: toward ordered bulk-heterojunction solar cells," *ACS Nano*, vol. 3, no. 6, pp. 1415–1422, 2009.

[12] J. Martín, J. Maiz, J. Sacristan, and C. Mijangos, "Tailored polymer-based nanorods and nanotubes by "template synthesis": from preparation to applications," *Polymer*, vol. 53, no. 6, pp. 1149–1166, 2012.

[13] R. O. Al-Kaysi, T. H. Ghaddar, and G. Guirado, "Fabrication of one-dimensional organic nanostructures using anodic aluminum oxide templates," *Journal of Nanomaterials*, vol. 2009, Article ID 436375, 14 pages, 2009.

[14] A. Kamarundzaman, M. S. Fakir, A. Supangat, K. Sulaiman, and H. Zulfiqar, "Morphological and optical properties of hierarchical tubular VOPcPhO nanoflowers," *Materials Letters*, vol. 111, pp. 13–16, 2013.

[15] M. S. Fakir, A. Supangat, and K. Sulaiman, "Templated growth of PFO-DBT nanorod bundles by spin coating: effect of spin coating rate on the morphological, structural, and optical properties," *Nanoscale Research Letters*, vol. 9, no. 1, p. 225, 2014.

[16] A. Supangat, A. Kamarundzaman, N. Asmaliza Bakar, K. Sulaiman, and H. Zulfiqar, "P3HT:VOPcPhO composite nanorods arrays fabricated via template-assisted method: enhancement on the structural and optical properties," *Materials Letters*, vol. 118, pp. 103–106, 2014.

[17] J. Martín, M. Hernández-Vélez, O. de Abril et al., "Fabrication and characterization of polymer-based magnetic composite nanotubes and nanorods," *European Polymer Journal*, vol. 48, no. 4, pp. 712–719, 2012.

[18] Z. L. Xiao, C. Y. Han, U. Welp et al., "Fabrication of alumina nanotubes and nanowires by etching porous alumina membranes," *Nano Letters*, vol. 2, no. 11, pp. 1293–1297, 2002.

[19] C. J. Collison, L. J. Rothberg, V. Treemaneekarn, and Y. Li, "Conformational effects on the photophysics of conjugated polymers: a two species model for MEH-PPV spectroscopy and dynamics," *Macromolecules*, vol. 34, no. 7, pp. 2346–2352, 2001.

[20] J. S. Kim, J. H. Lee, J. H. Park, C. Shim, M. Sim, and K. Cho, "High-efficiency organic solar cells based on preformed poly(3-hexylthiophene) nanowires," *Advanced Functional Materials*, vol. 21, no. 3, pp. 480–486, 2011.

[21] J. Y. Oh, M. Shin, T. I. Lee et al., "Self-seeded growth of poly(3-hexylthiophene) (P3HT) nanofibrils by a cycle of cooling and heating in solutions," *Macromolecules*, vol. 45, no. 18, pp. 7504–7513, 2012.

[22] T. Erb, U. Zhokhavets, G. Gobsch et al., "Correlation between structural and optical properties of composite polymer/fullerene films for organic solar cells," *Advanced Functional Materials*, vol. 15, no. 7, pp. 1193–1196, 2005.

[23] X. Zhang, H. Gorohmaru, M. Kadowaki et al., "Benzo-2,1,3-thiadiazole-based, highly dichroic fluorescent dyes for fluorescent host-guest liquid crystal displays," *Journal of Materials Chemistry*, vol. 14, no. 12, pp. 1901–1904, 2004.

[24] M. A. Stevens, C. Silva, D. M. Russell, and R. H. Friend, "Exciton dissociation mechanisms in the polymeric semiconductors poly (9,9-dioctylfluorene) and poly (9,9-dioctylfluorene-co-benzothiadiazole)," *Physical Review B: Condensed Matter and Materials Physics*, vol. 63, no. 16, Article ID 165213, 2001.

[25] U. Zhokhavets, T. Erb, H. Hoppe, G. Gobsch, and N. S. Sariciftci, "Effect of annealing of poly(3-hexylthiophene)/fullerene bulk heterojunction composites on structural and optical properties," *Thin Solid Films*, vol. 496, no. 2, pp. 679–682, 2006.

[26] D. Chirvase, J. Parisi, J. C. Hummelen, and V. Dyakonov, "Influence of nanomorphology on the photovoltaic action of polymer-fullerene composites," *Nanotechnology*, vol. 15, no. 9, pp. 1317–1323, 2004.